JOURNAL OF TECHNIQUES

Journal homepage: http://journal.mtu.edu.iq

RESEARCH ARTICLE - ENGINEERING

A Design of Fractal Hilbert MIMO Antenna for 5G Mobile

Noora Rafid Kamil[1*], Ahmed Ghanim Waddy[2], Aseel Hameed AL-Nakkash[1]

[1] Electrical Engineering Technical College, Middle Technical University, Baghdad, Iraq.

[2] Al-Furat Al-Awsat Technical University, Iraq.

[*] Corresponding author E-mail: noora.rafid94@gmail.com

Article Info.

Article history:

Received
17 December 2021

Accepted
31 January 2022

Publishing
31 March 2022

Abstract

This paper presented two new fractal Hilbert MIMO antenna designs with different two thicknesses (0.8mm and 1 mm) and used hybrid techniques between neutralization lines (NL) and defected ground structure (DGS), to enhance mutual coupling of the antenna for 5G applications. Higher isolation and smaller size are major advantages of this design. The proposed fractal Habrit curve MIMO antennas were fabricated for the 3800 - 5460 MHz and 3735-5390 MHz bands with a 49 dB and 40 dB return loss and high isolation of 19.67 dB and 18.5 dB, using FR4 with dimensions of (24 × 45 × 0.8mm^3) and (24 × 45 × 1mm^3) respectively. The results prove that the MIMO antenna is suitable for a sub-6 band that is qualified for 5G smartphone applications.

Keywords: ECC; Fractal; Hilbert; Isolation; MIMO Antennas.

1. Introduction

Recently, communication systems based on LTE as well as 5G, which require compact antennas at the user end (mobile device) are matter of interest for researchers [1-4]. The current work is focused on different antenna designs to further reduce the size and increase isolation for both LTE and 5G. One of the requirements to achieve good performance in a MIMO communication system is that the correlations between the signals, received by the MIMO antenna ports, should be sufficiently low. The signal correlation between antenna ports is often divided into two separate effects, the first due to channel correlation and the second due to the isolation between antenna elements. Although the two effects are not independent (the effect of mutual coupling will alter the antenna patterns and therefore the channel correlation), one can meaningfully think of the requirement for low signal correlation between antenna ports while requiring sufficiently low channel correlation and sufficiently good antenna isolation with low correlation coefficient in terms of diversity [1-3], [5].

A critical aspect in the design of MIMO antennas for communication systems is, therefore, providing sufficiently good antenna isolation. The design of compact MIMO antennas with good isolation is difficult to achieve as there are some fundamental design limits on the number of antennas that can be packed into a given size or area. The designs that come close to these limits are of interest. Previous works on MIMO antenna design demonstrated a large variety of approaches. Most of these approaches provide an isolation of 10-20dB between antennas. This isolation level has been shown enough for providing good increase in MIMO capacity [1-4]. The researchers Goraia et al., presented fractal Hilbert with dimension 30 × 41 × 1.59 mm^3 at resonant frequency 8.5 GHz. To enhance isolation 20 dB, ECC less than 0.1 and good efficiency 80% [6]. Other researchers Jeet B et al. have suggested a new fractal Hilbert MIMO antenna with 30.75 × 37.8 mm^2. The researchers achieved the isolation of less than 20 dB, ECC of less than 0.03 and efficiency of 72 %.[7]. A study by Gurjar et al., presented Sierpinski fractal MIMO antenna with two ports based on a monopole antenna. It used neutralization line technique of mutual coupling. It dimensions of the MIMO antenna 24 × 30 mm based on a Sierpinski slot unit monopole antenna results in isolation less than 16.3 dB [8].

Nomenclature & Symbols			
MIMO	Multiple Input Multiple Output	dB	decibel
NL	Neutralization Lines	ECC	Envelope Correlation Coefficient
5G	Fifth-Generation	SMA	SubMiniature version A
DGS	Defected Ground Structure	CST	Computer Simulation Technology
fr	frequency		

This paper provides a new contribution to compact MIMO antenna designs. The contribution focused on the design new of a Hilbert slot MIMO antenna design for 5G application, which helps to achieve high isolation of MIMO elements, high efficiency and the low envelope correlation coefficient.

2. Geometry of Fractal Hilbert Antenna

The process of the proposed design was a fractal Hilbert antenna composed of two process stages. In the first stage, designing a single antenna. Secondly, combining two single antennas to form a MIMO antenna. After selection of the geometrical parameters for the desired MIMO antennas, the antenna models were simulated by the CST program. The dimensions of the parameters were optimized by CST to get the optimal results with required specifications of MIMO antennas.

2.1. Single Antenna Structure

The single antenna proposed is a rectangular antenna which was designed through a procedure consisting of two stages. Firstly stage, a rectangular-shaped antenna was designed with dimensions of 24× 21.5 mm^2. Secondly stage, adding slots Hilbert-shaped for it, as shown in Fig.1. The operating frequency of the patch was calculated through Equation (1) [9]:

$$f_r = \frac{c}{2L\sqrt{\epsilon_r}} \quad (1)$$

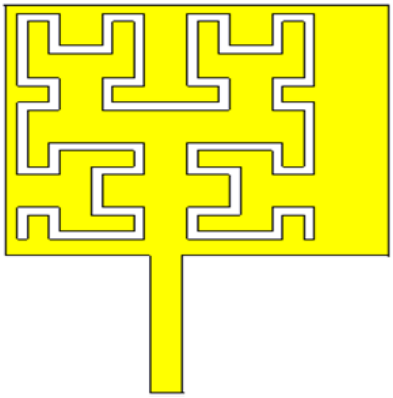

Fig 1. Configuration process of the Hilbert antenna

The features of fractal geometry are: Firstly, miniaturization which leads to satisfy the needs for recent wireless systems. Secondary, improve the performance of single antenna in term of radiation efficiency, bandwidth, and gain, Thirdly, reduced mutual coupling in the fractal antenna array. Finally, more reliable and cheaper as compared with traditional. On other hand, the drawback of fractal geometry is complex design (some kinds are difficult to design). Also, the advantage of fractal starts to decrease after several iteration numbers for some designs. Because of, the features offered by the fractal geometry are more than its drawbacks and the development of the computational techniques and computer technologies have an important role to make these drawbacks less effective [10-12].

The Hilbert curve geometry with four iterations is illustrated in Fig.2, it is clear that the initiator is indicated at k=1while the generator is indicated at k=2 which represent the 2nd iteration. the idea of Hilbert curve geometry is implemented by making four copies of the previous iteration to produce the next iteration with using additional line segment for connection these copies together. The number of lines for the (1st iteration) was 3 line. Then, the number of lines for (2^{nd} iteration) was 15 line and for (3^{rd} iteration) was 63 line. Equation (2) can be used to calculate the number of lines of the iterations [10-12].

$$No.of\ lines = 2^{dk} - 1 \quad \text{Where d=2, k = number of iterations 1,2,3,4…} \quad (2)$$

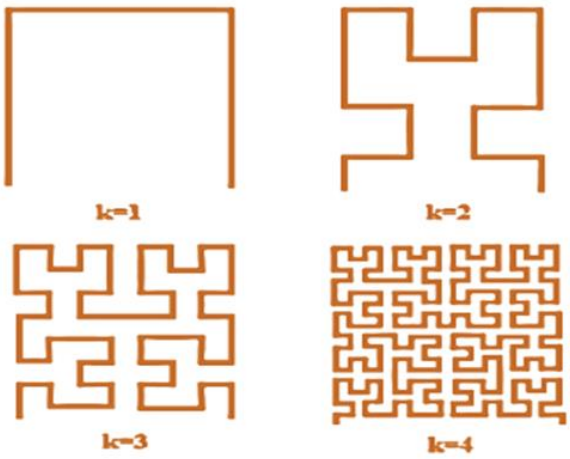

Fig 2. The generation of Hilbert curve [12]

2.2. MIMO Antenna Design

In Fig. 3, The proposed Hilbert MIMO antenna proposed includes two separate ports with a distance less than 2 mm, monopoles printed on a 24 × 45 mm FR-4 substrate with a dielectric constant of 4.3 and a thickness of 1mm. The dimensions of the proposed MIMO antenna are mentioned in Table 1. Radiating elements of the two-element MIMO antenna design have a symmetric monopole antenna. The dimensions and location of the feed point were optimized to get the best possible impedance, in a match to the antenna. The microstrip patch antenna can be fed using different methods including microstrip aperture coupling, line feed, coaxial probe feed, electromagnetic coupling, and coplanar waveguide. The proposed MIMO antenna using the feed line antenna is shown in Fig.3. The designed structure was fed using a (50 Ω) microstrip patch feed-line with the width of (Wf) and length of (Lf). During the simulations, a coaxial connector, SMA, was connected to the feed line to get the results closest to real-time. The width of the feed line and the microstrip patch substrate were fixed to achieve a 50 Ω impedance at Wf = 1.477 mm.

On ground plane of the substrate, design utilizes as well a U-shaped incision with the line-shaped insertions with circle slots redia are c1=1 mm and c2=2 mm in the ground substrate to enhancement to isolation between elements of antennas. The impedance match of the proposed antenna was also enhanced by cutting a rectangular slot around the microstrip line on the ground plane which was located at the back of the substrate. addition that, inserted vertical line of length 24 mm and width L1 = 1 mm to obtain high isolation.

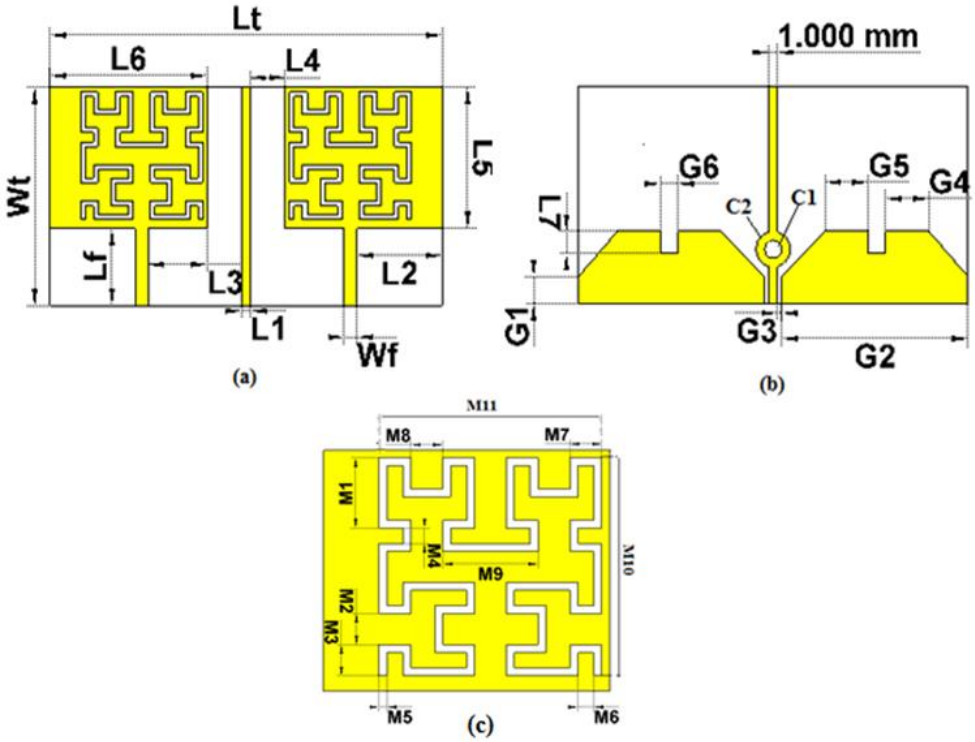

Fig 3. Proposed Hilbert Fractal MIMO antenna, (a) Patch plane, (b) Ground plane and (C) Hilbert slot

Table 1 Dimensions of the Parameters of Hilbert MIMO Antenna(mm)

Parameters	L1	L3	L5	L7	G1	G2
Dimensions	1	6.762	15.5	2.5	3	21.5
Parameters	L2	L4	L6	G3	G4	G5
Dimensions	9.762	4.132	18	5	5	5
Parameters	G 6	C1	C2	Wt	Lt	Wf
Dimensions	2	1	2	24	45	1.477
Parameters	Lf	ht	hs	M 1	M 2	M 3
Dimensions	8,5	0.0035	1	4.5	2	2
Parameters	M4	M5	M6	M7	M8	M9
Dimensions	1	0.5	1	2	2	6
Parameters	M 10	M 11	-	-	-	-
Dimensions	14	14	-	-	-	-

3. Results and Discussion

3.1. Single Antenna

The single of the antenna design was a fractal Habrit curve with procedure offered in four steps. The first step, a rectangular shape antenna (iteration 0) was designed with dimensions of 24 × 21.5 mm^2 with dimensions of patch antenna 18 × 15.5 mm2 as shown in Fig. 3. Secondly step, the rectangular-shape antenna was changed to add U-shape slot (iteration 1) with dimensions of slot antenna 14 × 14 mm^2 as shown in Fig. 4. In the third to fourth steps, add Habrit curve (iteration 2 and iteration 3). The return loss for the four antennas is presented in Fig. 3, we observed the return loss increase in iteration 3 (20 dB) at the band (4000- 5512 MHz).

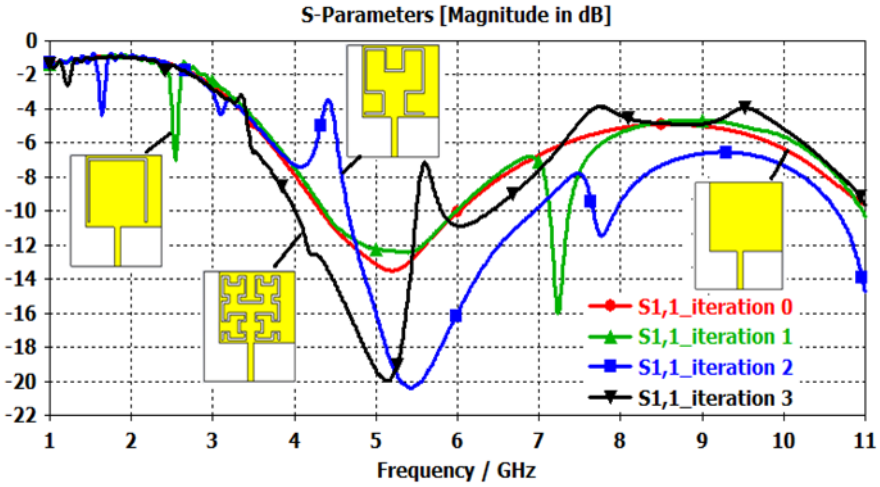

Fig 4. Reflection coefficient for four antennas

3.2. MIMO Antenna

The simulation to S-parameters S11and S12 was employed to investigate the results of changing the dimensions of radiating elements Habrit curve iteration 0, iteration1, iteration 2, iteration 3 and thickness of hs parameter.

Effect of the Habrit curve and thickness hs: Fig. 5 (a) show a design without Habrit curve (iteration 0). The first iteration (see Fig. 5 (b)) was created with integration of two patch antennas and adding a U-shape slot to each of them. The next iteration (see Fig. 5 (c)) was made by using Equation 2 of the changed patch of antenna1 to configure antenna 2, the same process was used in the 3rd iteration (see Fig. 5 (d)).

The varying thickness of the substrate (hs = 0.8) mm and making other radiation elements lead to the results of MIMO design change. Zero iteration, the solid curve displays S-parameters (S11) of antenna when thickness of the substrate (hs=0.8mm). An isolation value of 17.5dB and a return loss of 38dB was observed with operating band 3806 - 5879 MHz, as shown in Fig. 6 (a). By changing the thickness of the substrate hs = 1mm, the simulations explained the S-parameters were S11=18.72 dB and S22=18.4 dB with operating band 3736 - 5652 MHz, as shown in Fig. 6 (b).

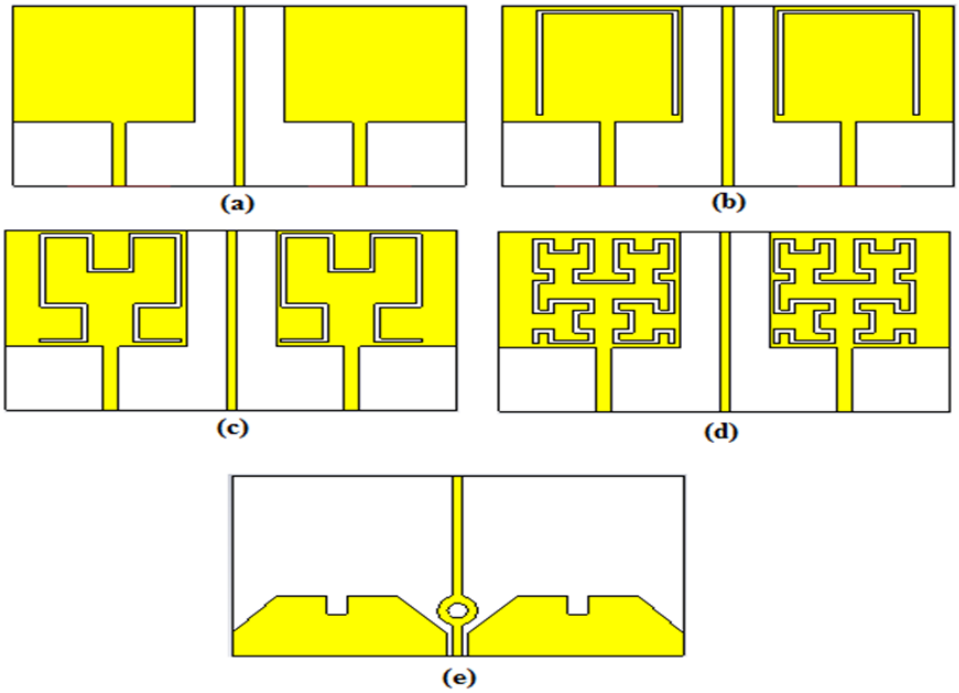

Fig 5. Prototype fractal Habrit curve MIMO antenna; (a) Front view of zero iteration, (b) Front view of first iteration, (c) Front view of second iteration, (d) Front view of third iteration, (e) Bottom view

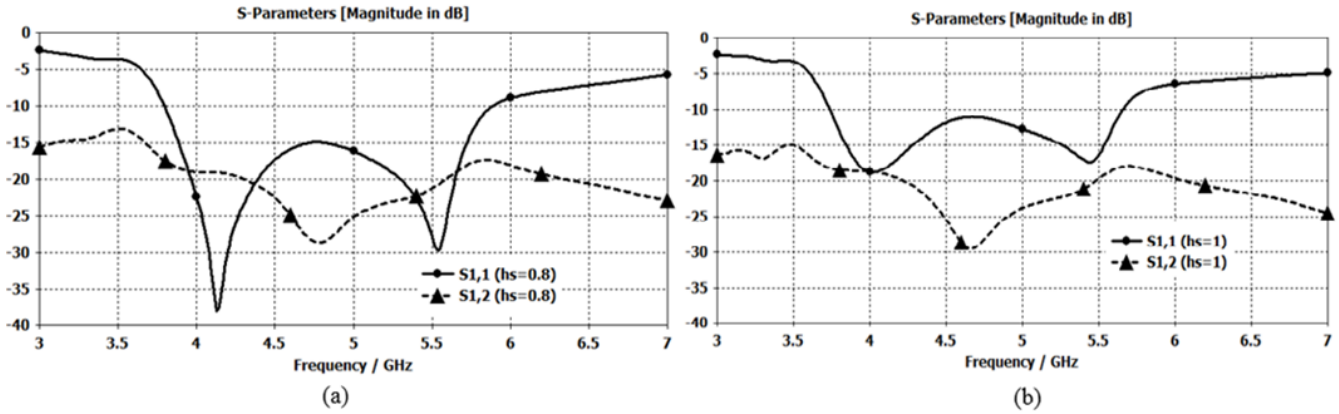

Fig 6. S parameters of Habrit curve MIMO-antenna 0th iteration; (a) When hs=0.8mm, (b) When hs=1mm

Fig. 7 presents the first iteration if (hs=0.8mm) than isolation value is17dB and the return loss is 25.5dB, with the operating band being 3767 - 5969 MHz. When changing (hs=1mm), the resulting operating band was 3712 - 5719 MHz with S11=16.46dB and S12=17.68dB, as shown in Fig. 7 (b).

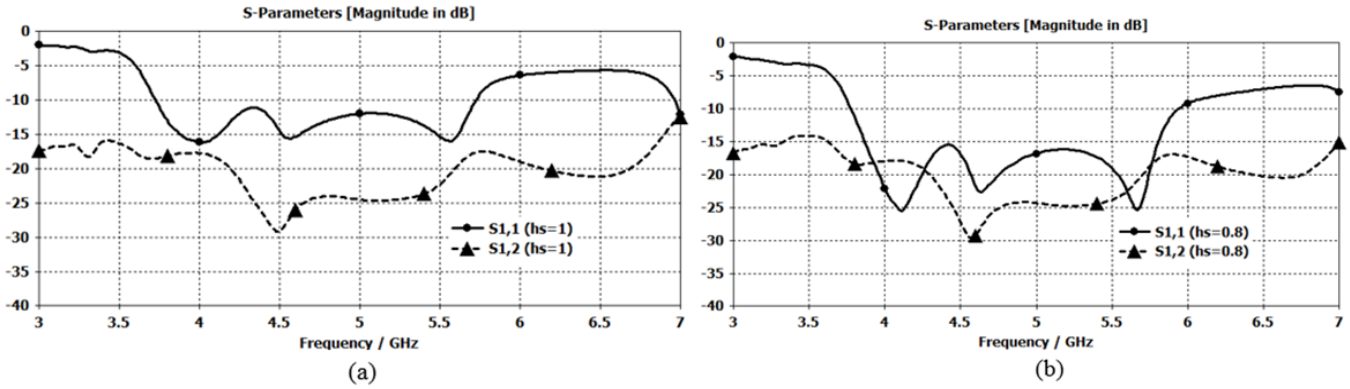

Fig 7. S-parameters of Habrit curve antenna 1st iteration; (a) When (hs=0.8mm), (b) When (hs=1mm)

In the Second iteration, when using hs=0.8mm, the simulations showed a single operating band 3777 - 4220 MHz with S11=32.85dB and S12=15dB, as shown in Fig.8 (a). While Fig.8 (b) shows the results which using thickness of the substrate hs=1mm, which change of operating band to 3735 - 4081 MHz and increase the isolation to 16.65 dB with the return losses dropped to 22.28dB.

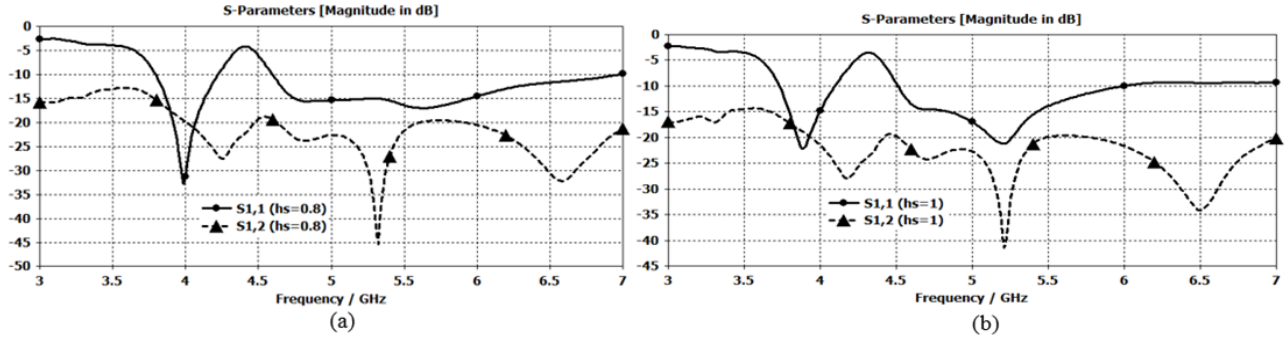

Fig 8. S-parameters of Habrit curve MIMO antenna 2nd iteration; (a) When (hs=0.8mm), (b) When (hs=1mm)

By changing the thickness of hs=0.8mm, the simulations showed (third iteration) operating band 3800- 5460 MHz, S11=49 dB and S12=19.67dB, as shown in Fig. 9 (a). While, when using the thickness of substrate hs=1mm, the operating band was changed to 3768 - 5390 MHz, S12 was decreased to 18.5dB and S11 was decreased to 40dB, as shown in Fig. 9 (b). The effects of a slot Habrit curve was increased isolation (19.67 dB and 18.5 dB) and return loss (49 dB and 40 dB) to both thicknesses 0.8 mm and 1mm respectively.

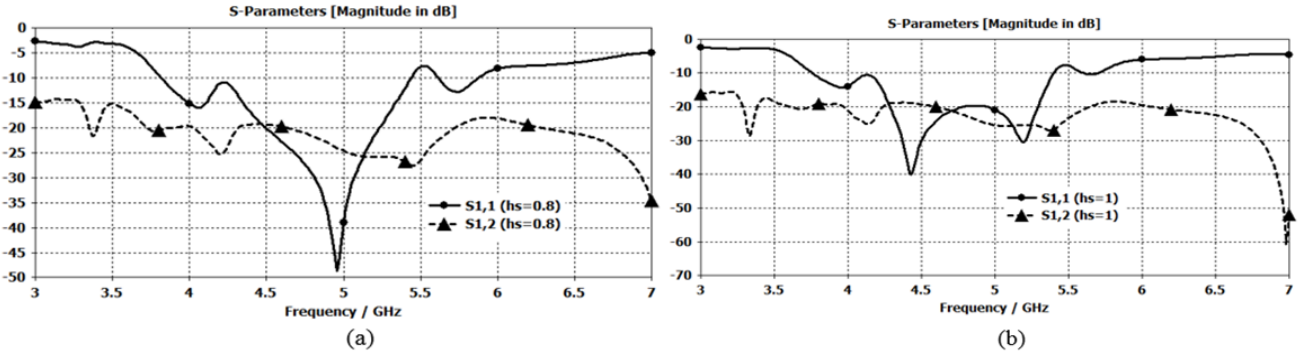

Fig 9. S-parameters of Habrit curve MIMO antenna 3rd iteration (a) When (hs=0.8mm) (b) When (hs=1mm)

3.3. MIMO Antenna

As discussed earlier the adoption of NL and DGS techniques for MIMO antenna decreases mutual coupling between the ports from 10 dB to 19.76 dB and 18.5 dB for both thicknesses 0.8 mm and 1 mm respectively. Fig. 10 and Fig. 11 shows a MIMO antenna without and with techniques of isolation if (hs=0.8 mm and hs=1mm) respectively.

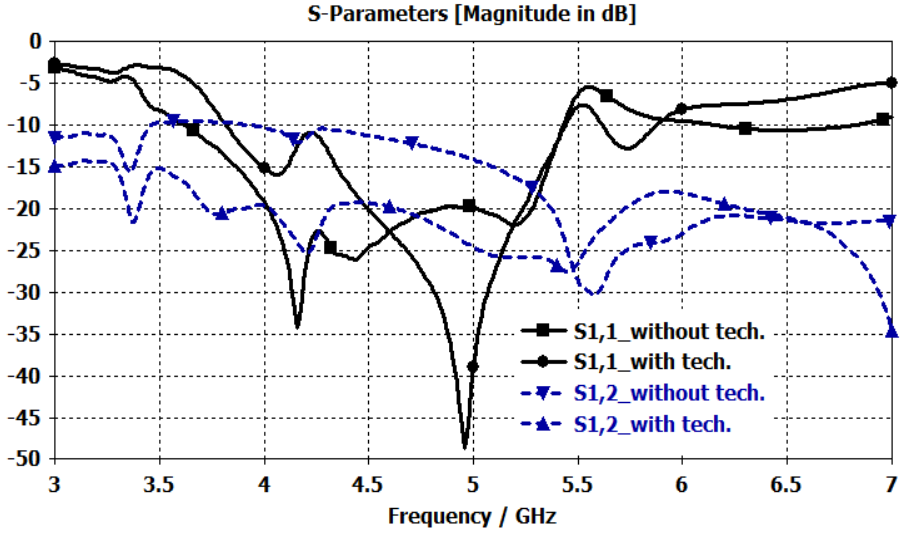

Fig 10. Effect comparison with and without hybrid technique of MIMO antenna when thickness (hs=0.8mm)

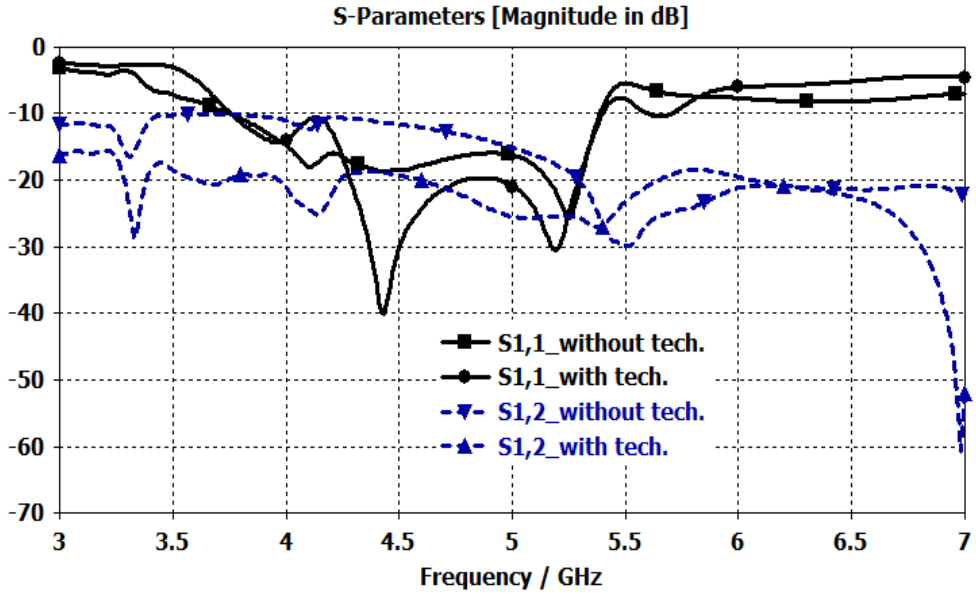

Fig 11. Effect comparison with and without hybrid technique of MIMO antenna when thickness (hs=1mm)

Fig. 12 shows the effect of isolation techniques with fractal hybrid slots was embedded, where notes that surface-current was often centred-around slots in opposite directions. we observed that antenna has more effect when hs=1mm, where focused surface-current about slots for both patch plane and ground plane.

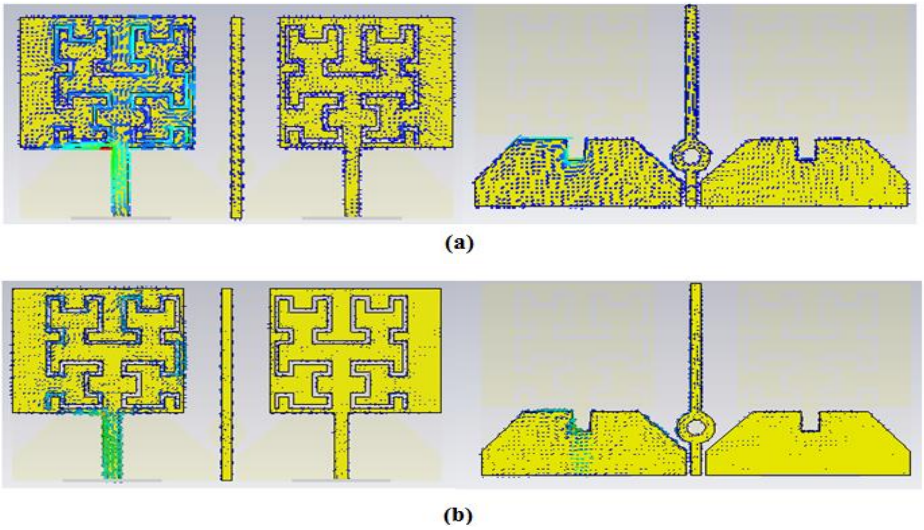

Fig 12. Current densities of port1 of fractal antenna; (a) when (hs= 1mm), (b) when (hs= 0.8mm)

3.4. Radiation Pattern

Fig. 13 displays the radiation pattern of MIMO antenna when (hs=0.8mm and hs=1mm) without and with techniques at centre frequency 4.96 Hz respectively.

3.5. ECC and Efficiency

This portion discusses the ECC of the fractal hybrid MIMO antenna. When dimensions of the slot fractal Hybrid curve were changed, maximum ECC obtained was (0.0177, 0.004, 0.001 and 0.0047) and (0.015, 0.02, 0.017and 0.0034) for the four iterations (zero, 1, 2, and 3) for both thickness 1 mm and 0.8 mm respectively. A good efficiency (41-65%) and (41-65%) were obtained of the particular operating bands, Table 2 shows ECC and the efficiency values by changing the fractal hybrid slot.

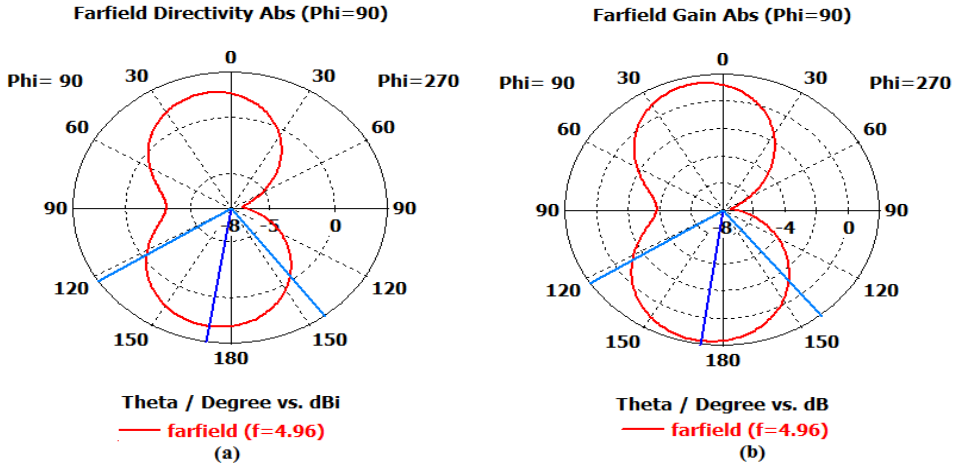

Fig 13. Radiation pattern of MIMO antenna at center frequency 4.96 GHz; (a) When (hs=0.8mm), (b) When (hs=1mm)

Table 2 Summary of efficiency with ECC of fractal Hybrid antenna (hs=1mm and hs=0.8 mm)

Number of iterations	0.8 mm		1 mm	
	ECC	Eff. %	ECC	Eff.%
0 iteration	0.015	45-80	0.0177	45-78
1 iteration	0.02	45-78.2	0.004	43-74
2 iteration	0.017	47-55.9	0.001	44-51
3 iteration	0.0034	41-67.9	0.0047	41-65

3.6. Prototype and measurement

The proposed fractal Habrit curve MIMO antennas were fabricated for the 3800 - 5460 MHz and 3735-5390 MHz bands with a return loss about of values (49 dB and 40 dB) and isolation of (19.67 dB and 18.5 dB) respectively, , using FR4 with dimensions of ($24 \times 45 \times 0.8mm^3$) and (24 × 45 × 1mm3), as shown in Fig. 14.

Fig. 15 shows simulated and measured s-parameters (S11 and S12), described through the two typical antennas. The antenna fabrication has given measured isolation 19.58 dB and 10.5 at operating bands and a return loss of 31dB and 22 dB. We note a difference in return loss for two thicknesses, this difference is normal because of the inaccuracy of etching or cutting processes or soldering processes.

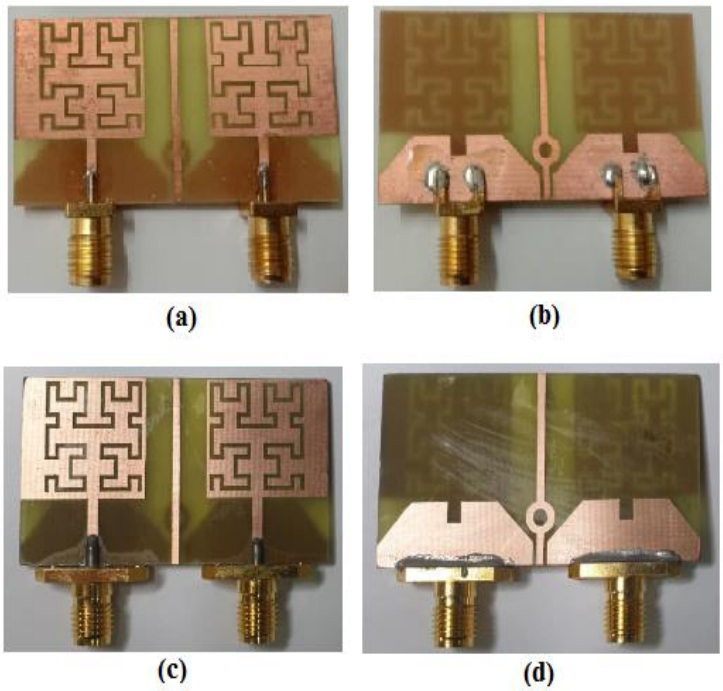

Fig 14. Prototypes Habrit MIMO antenna; (a) Patch plane when thickness the substrate (hs=0.8 mm), (b) Ground plane when thickness the substrate (hs=0.8 mm), (c) Patch plane when thickness the substrate (hs=1 mm), (d) Ground plane when thickness the substrate (hs=1 mm)

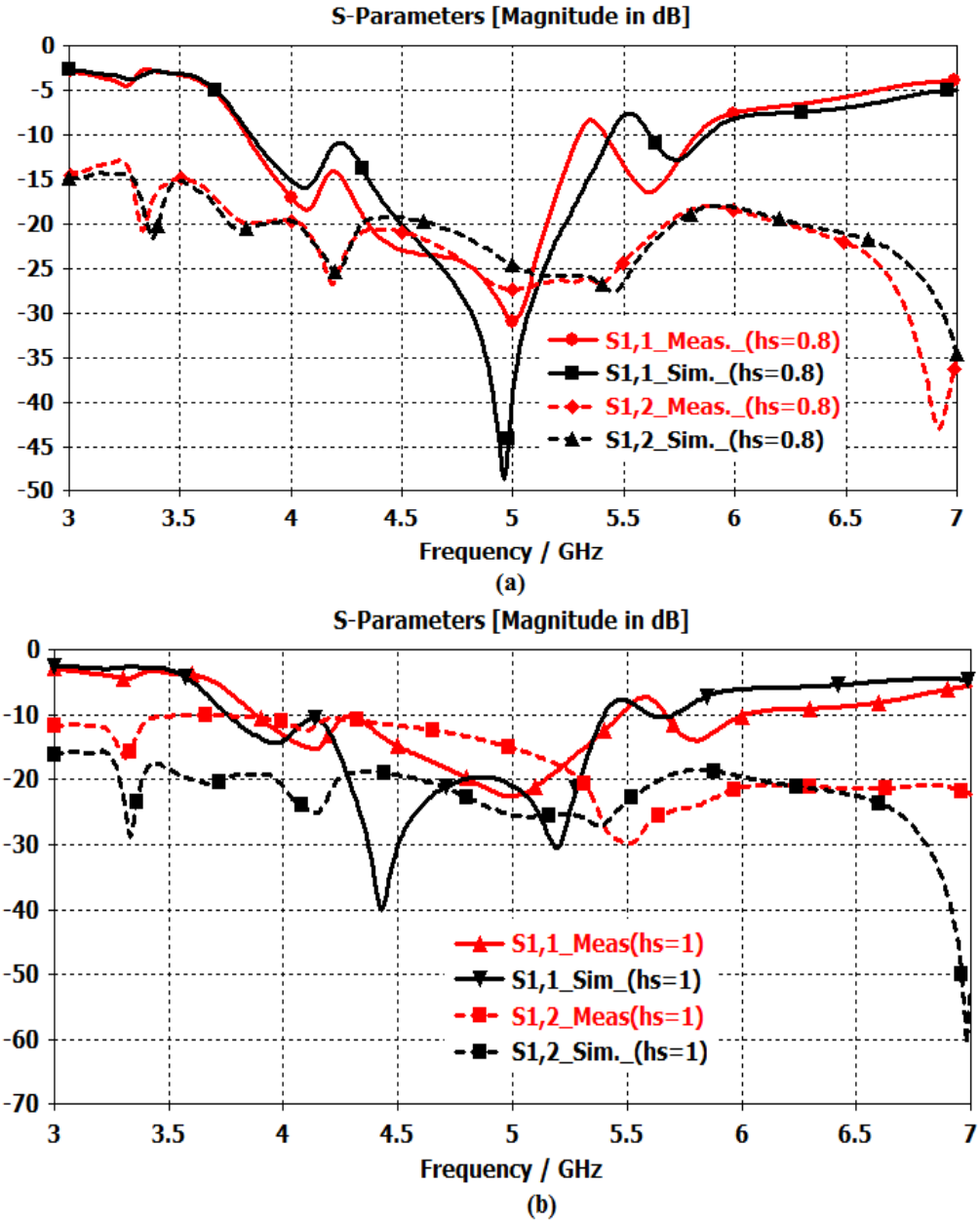

Fig 15. S-parameters; (a) When (hs=0.8mm), (b) When (hs=1mm)

Table 3 provides a comparison between fractal Habrit curve MIMO antenna and other previous related. The findings show that fractal Habrit curve MIMO antenna has excellent isolation with a smaller size. Also, the operating band of the proposed antenna can be used for 5G applications. In this design, a method for designing two MIMO antennas using a fractal habrit curve was presented, which helps to achieve small size ($24 \times 45 \times 0.8$ mm^3 and $24 \times 45 \times 1$ mm^3) and high isolation 19.67 dB and 18.5 dB. Higher isolation and smaller size are major advantages of this design over the previous designs.

Table 3 Comparison between another research works and the proposed antenna

Ref	Bandwidth (MHz)	Size (mm2)	Isol.	ECC	Eff (%)	DT
[13]	(4030 – 5400)	77.6 × 63	13	< 0.15	(86 – 92)	DN
[14]	(3100 – 5000)	400 × 400	20	< 0.002	> 68	NL
[15]	(3600 – 4200)	26 × 46	15	< 0.003	(78 – 90)	DGS and NL
[16]	(3900 –4200)	40.5×40.5	17	< 0.035	(40 – 80)	DGS and DN
[17]	(3600–3990)	37 × 56	15	< 0.08	(49 – 83)	NL
[18]	(3300 – 4200)	150 × 200	10	< 0.1	(60 – 80)	NL
This work	(3800 – 5460) (3735-5390)	24 × 45	19.67	< 0.004	(41 – 65)	DGS and NL

4. Conclusion

This paper focused on the design along analysis of MIMO fractal antenna. Computer system technology (CST) was used to optimize the dimensions of the proposed antennas and for analyzing the radiation characteristics. The measured characteristics of fabricated prototypes were compared with simulated data and a notable agreement was observed between them. All proposed antennas have easy fabrications because of use of FR-4 material. Notwithstanding small area of proposed antennas compared with several of the survey MIMO antennas presented this paper has characteristics of high isolation, very small size, low ECC, efficiency and easy fabrication; and thereby making them suitable for 5G communications.

Acknowledgement

I'd want to express my gratitude and appreciation to my supervisor Assist Prof. Dr. Aseel Hameed for her reviews and my co-supervisor Prof. Dr. Ahmed Ghanim for his insights and comments.

Reference

[1] Y. Li and C. Sim.: "12-Port 5G Massive MIMO Antenna Array in Sub-6GHz Mobile Handset for LTE Bands 42 / 43 / 46 Applications," IEEE Access, vol. 6, pp. 344–354, (2018).
[2] I. Nadeem and D. Y. Choi.: "Study on Mutual Coupling Reduction Technique for MIMO Antennas," IEEE Access, vol. 7, pp. 563–586, (2019).
[3] A. C. J. Malathi and D. Thiripurasundari.: "Review on Isolation Techniques in MIMO Antenna Systems," Indian J. Sci. Technol., vol. 9, no. September, (2016).
[4] R. Khan, S. Member, M. R. Kamarudin, and S. Member.: "User Influence on Mobile Terminal Antennas: A Review of Challenges and Potential Solution for 5G Antennas," IEEE Access, vol. 6, pp. 77695–77715, (2018).
[5] H. Zou, Y. Li, C. Y. D. Sim, and G. Yang.: "Design of 8 × 8 dual-band MIMO antenna array for 5G smartphone applications," Int. J. RF Microw. Comput. Eng., vol. 28, no. 9, pp. 1–3, (2018).
[6] A. Gorai, A. Dasgupta, and R. Ghatak, "A compact quasi-self-complementary dual band notched UWB MIMO antenna with enhanced isolation using Hilbert fractal slot," AEU - Int. J. Electron. Commun., vol. 94, no. December 2017, pp. 36–41, (2018).
[7] J. Banerjee, A. Gorai, and R. Ghatak, "Design and analysis of a compact UWB MIMO antenna incorporating fractal inspired isolation improvement and band rejection structures," AEU - Int. J. Electron. Commun., vol. 122, p. 153274, (2020).
[8] Gurjar, R., Upadhyay, D.K., Kanaujia, B.K. and Kumar, A.: "A compact modified sierpinski carpet fractal UWB MIMO antenna with square-shaped funnel-like ground stub," AEU-International Journal of Electronics and Communications, 117, p.153126, (2020).
[9] C. A. Balanis.: "ANTENNA THEORY ANALYSIS AND DESIGN," John Wiley, (2016).
[10] J. L. Ramírez and G. N. Rubiano.: "Biperiodic fibonacci word and its fractal curve," Acta Polytech., vol. 55, no. 1, pp. 50–58, (2015).
[11] M. F. Mokbel and W. G. Aref.: "Space-Filling Curves," Encycl. Database Syst., no. c, pp. 2674–2675, (2009).
[12] A. R. Butz.: "Convergence with Hilbert's space filling curve," J. Comput. Syst. Sci., vol. 3, no. 2, pp. 128–146, (1969).
[13] Y. F. Cheng, X. Ding, W. Shao, and B. Z. Wang.: "Reduction of Mutual Coupling Between Patch Antennas Using a Polarization-Conversion Isolator," IEEE Antennas Wirel. Propag. Lett., vol. 16, pp. 1257–1260, (2017).
[14] W. A. E. Ali and A. A. Ibrahim.: "A Compact Double-Sided MIMO Antenna with an Improved Isolation for UWB Applications," AEUE - Int. J. Electron. Commun., 2017.
[15] A. M. Ibrahim, I. M. Ibrahim, and N. A. Shairi.: "Compact MIMO antenna with high isolation for 5G smartphone applications," J. Eng. Sci. Technol. Rev., vol. 12, no. 6, pp. 121–125, 2019, doi: 10.25103/jestr.126.15.
[16] I. Suriya and R. Anbazhagan.: "Inverted-A based UWB MIMO antenna with triple-band notch and improved isolation for WBAN applications," Int. J. Electron. Commun. (AEÜ), vol. 99, pp. 25–33, (2019).
[17] S. Chouhan, V. S. Kushwah, D. K. Panda, and S. Singhal.: "Spider-shaped fractal MIMO antenna for WLAN/WiMAX/Wi-Fi/Bluetooth/C-band applications," AEU - Int. J. Electron. Commun., vol. 110, p. 152871, 2019, doi: 10.1016/j.aeue.2019.152871.
[18] K. L. Wong, B. W. Lin, and S. E. Lin.: "High-isolation conjoined loop multi-input multi-output antennas for the fifth-generation tablet device," Microw. Opt. Technol. Lett., vol. 61, no. 1, pp. 111–119, (2019).